



Substituent effect on benzylic lithiation of sulfides. Synthesis of diboronic acids derived from aryl–alkyl sulfides



Marek Dąbrowski^a, Krzysztof Durka^a, Tomasz Kliś^{a,*}, Janusz Serwatowski^a, Krzysztof Woźniak^b

^a Warsaw University of Technology, Faculty of Chemistry, Noakowskiego 3, 00-664 Warsaw, Poland

^b Warsaw University, Faculty of Chemistry, Pasteura 1, 02-093 Warsaw, Poland

ARTICLE INFO

Article history:

Received 25 September 2012
Received in revised form 8 February 2013
Accepted 22 February 2013
Available online 26 February 2013

Keywords:

Lithiation
Boronic acids
Sulfides
Hammett equation
Ab initio calculations

ABSTRACT

The relative benzylic deprotonation rate constants of aryl–benzyl sulfides have been measured and the obtained values were compared with the substituent constants using the Hammett equation and with deprotonation Gibbs energies calculated on B3LYP/aug-cc-pVDZ level. The deprotonation rate depends on the stabilization of the negative charge, which is spread over the benzene ring. The series of brominated aryl–benzyl sulfides was di-lithiated by Br/Li exchange using *t*-BuLi and the obtained organolithium compounds were converted into the respective diboronic acids. Lithiation of aryl–benzyl sulfides containing a bromine atom in the *para* or *ortho* positions occurs selectively, however for the *meta* derivative, the process is plagued by competitive benzylic deprotonation. This fact can be rationalized on the basis of the obtained relative deprotonation rate constants. The X-ray analysis of bis-(2-dihydroxyborylphenylthio)methane revealed the existence of three different structural motifs, which stabilize the structure by hydrogen bonding formation.

© 2013 Elsevier Ltd. All rights reserved.

1. Introduction

Boronic acids are reactive intermediates, which take part in many valuable reactions in organic synthesis.¹ Recently there has been significant interest in the application of diboronic acids as the components of polymeric porous materials for gas absorption.² Although the first results of these studies are promising, the broad range of diboronic acids needs to be tested to obtain high quality materials. In this work we describe an effective method to prepare diboronic acids by di-lithiation of aryl–benzyl sulfides. However, the stabilizing effect of sulfur may result in the lowering of the lithiation selectivity as a result of competitive deprotonation at the aliphatic position.³ Our recent studies revealed that this process is especially important in the lithiation of aryl–benzyl sulfides,⁴ but can also become dominant in the lithiation of aryl–benzyl ethers containing an electronegative substituent in the phenyl ring.⁵ Thus, we decided to precede the preparation of diboronic acids with kinetic studies. The relative rate constants for the benzylic deprotonation of substituted aryl–benzyl sulfides were correlated with the structure using the Hammett equation. The obtained results were next compared with the deprotonation

Gibbs energy obtained using quantum-chemical calculations performed on B3LYP/aug-cc-pVDZ level of theory.

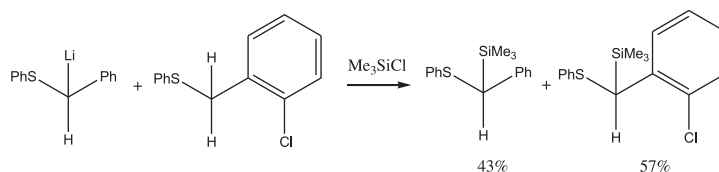
2. Results and discussion

2.1. Kinetic experiments

In order to perform the kinetic studies we decided to apply the protocol where the THF solution containing 1 equiv of benzyl–phenyl sulfide BPS (used as the reference) and 1 equiv of substituted benzyl–phenyl sulfide XBPS was treated at $-78\text{ }^{\circ}\text{C}$ with 1 equiv of LDA in the presence of excess $(\text{CH}_3)_3\text{SiCl}$ as the in situ electrophile. This procedure consisted of two steps, which involved benzylic deprotonation of the starting material followed by the reaction of the obtained benzyllithium derivative with an electrophile. In order to apply this methodology successfully, the deprotonation should be the rate determining step and the formed benzyllithiums cannot undergo any side reactions. Our initial experiments revealed that addition of (2-chlorobenzyl)phenyl sulfide to the solution of α -(phenylthio)benzyllithium followed by silylation with Me_3SiCl afforded the mixture of silylated sulfides (Scheme 1).

We believed that determination of the isotope effect could provide some evidence concerning the stability of benzyllithiums obtained after deprotonation. Thus, in the lithiation of **1**, an

* Corresponding author. Tel.: +48 22 2347575; fax: +48 22 6282741; e-mail address: ktom@ch.pw.edu.pl (T. Kliś).

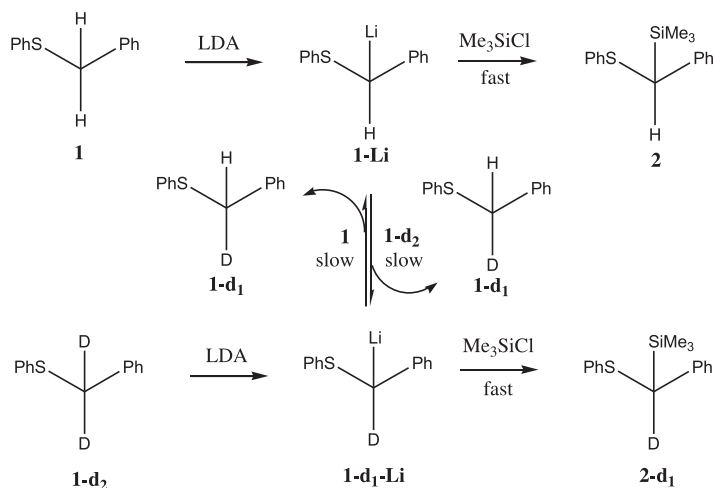


Scheme 1. Equilibration between benzyl–phenyl sulfides. Reaction conditions: THF, $-78\text{ }^{\circ}\text{C}$, Me_3SiCl quench after 0.5 h.

intermolecular isotope effect was measured for the reaction of **1** and **1-d₂** by the ratio of conversion of **1** to **2** and **1-d₂** to **2-d₁** upon reaction with a deficient amount of LDA and an excess of Me_3SiCl as the in situ electrophile (Scheme 2). The integration of the ^1H NMR spectrum obtained after the hydrolytic workup of the reaction mixture ($\text{CH}_{\text{benzylic}}$ 4.00 ppm, $-\text{Si}(\text{CH}_3)_3$ 0.14 ppm) revealed that the signals ratio corresponds with the selective formation of **2**. In our experiment, little deuterium was removed from **1-d₂**, rendering the precise measurement of the amount of **2-d₁**. The non-measurable concentration of **2-d₁** in the reaction mixture suggests that the intermolecular isotopic effect is very high, however, using ^1H NMR spectroscopy the quantitative evaluation is not possible. This result is in agreement with the one-step mechanism of the lithiation via a single transition state.⁶ The intermolecular isotope effect was next examined using the sequential procedure where the equimolar mixture of **1** and **1-d₂** was reacted with a deficient amount of LDA at $-78\text{ }^{\circ}\text{C}$. However, the quench with Me_3SiCl was conducted after 5 min. Interestingly, in this case the amount of **2-d₁** increased significantly. The ratio of **2/2-d₁**=10.3 can be rationalized on the basis of the equilibration between **1-Li** and **1-d₂**, which results with the formation of **1-d₁-Li** and **1-d₁**. The fact that **2-d₁** was not detected in the reaction with Me_3SiCl as the in situ electrophile suggests that the equilibration process is slower than the quench with Me_3SiCl .

$$\left(\frac{k_x}{k_h}\right) = \left(\frac{c_h}{c_x}\right) \left(\frac{c_x^0 - c_x}{c_h^0 - c_h}\right) \quad (1)$$

The relatively large positive ρ value indicates that electrons are moved toward the benzene ring in the transition state. This effect corresponds with the stabilization of the benzylic carbanion formed in the rate determining step. The rate of deprotonation is a result of the competition between the inductive and conjugative effect caused by the substituent. The highly electronegative fluorine atom is the σ acceptor, however, it acts simultaneously as a π -donor, and the resonance structure carrying the negative charge at the carbon atom bonded to fluorine does not contribute much to the electronic delocalization. Thus, the effect caused by a fluorine atom in the *para* position is responsible for the lowering of the rate of deprotonation in comparison to the derivative containing a fluorine atom in the *meta* position where only σ polarization works.¹⁰ The interplay between the acceptor properties of fluorine and the lone pair/lone pair repulsion is evident for the *ortho* isomer, for which rate of deprotonation is retarded by 50% in comparison to the *meta* derivative and increased drastically in comparison to the *para*-compound. On the other hand, the donation of π -electron density from heavier halogens is much weaker (poor π - n overlap): as a result the rate of deprotonation for *para*-halogenated derivatives increases in the following order: $k_{\text{F}} < k_{\text{Cl}} < k_{\text{Br}}$. The effect of



Scheme 2. Competitive reactions of benzyl–phenyl sulfide **1** and dideuterated benzyl–phenyl sulfide **1-d₂** with LDA and Me_3SiCl .

Once more, competition kinetic measurements were carried out to determine the relative rate constants of the benzylic deprotonation. In order to calculate the relative rate constants between XBPS and BPS (k_x/k_h), the second order kinetic equation was applied⁷ (Eq. 1) where c_{0x} and c_{0h} are the initial concentrations of XBPS and BPS, respectively, and c_x and c_h are the remaining concentrations of XBPS and BPS. The calculated values of the relative rate constants are collected in Table 1. The correlation between $\lg(k_x/k_h)$ and substituent constants (σ)⁸ can be approximated with the straight line (Fig. 1) with the gradient $\rho=3.9$.⁹

π - n overlap exhibited by the $-\text{OCH}_3$ group in the *para* position is especially high resulting in a deprotonation rate lower than that for reference compound. On moving the $-\text{OCH}_3$ group to the *meta* position, the π - n interaction is impeded and only the weak negative inductive effect works. The $-\text{CF}_3$ group is a potent σ and π acceptor, however, it is much more effective as a long range electron withdrawing substituent.¹¹ The effect of the $-\text{CF}_3$ group on deprotonation is highest for the *para*-isomer, whereas the rates of deprotonation for the *meta* and *ortho* isomer are retarded by 40% and 80%, respectively. In the case of the *meta* isomer only the

Table 1

Relative rate constants k_x/k_h calculated with the amounts of two competing substrates ($x=\text{PhSCH}_2(\text{XC}_6\text{H}_4)$, $h=\text{PhSCH}_2\text{C}_6\text{H}_5$) after their simultaneous reaction with LDA and Me_3SiCl in situ in THF at -78°C and deprotonation enthalpies and Gibbs energies [in kcal mol^{-1}] calculated in the framework of the B3LYP density functional

Aryl–benzyl sulfide	k_x/k_h	$\Delta\text{H}/\text{kcal mol}^{-1}$	$\Delta\text{G}/\text{kcal mol}^{-1}$
PhSCH ₂ (4-FC ₆ H ₄)	1.7	389.9	382.1
PhSCH ₂ (3-FC ₆ H ₄)	18.8	386.4	378.7
PhSCH ₂ (2-FC ₆ H ₄)	9.5	387.5	379.8
PhSCH ₂ (4-ClC ₆ H ₄)	13.4	387.6	379.8
PhSCH ₂ (3-ClC ₆ H ₄)	36.3	387.2	379.5
PhSCH ₂ (2-ClC ₆ H ₄)	23.7	386.4	378.7
PhSCH ₂ (4-BrC ₆ H ₄)	15.2	385.7	378.0
PhSCH ₂ (3-BrC ₆ H ₄)	64.3	386.3	378.6
PhSCH ₂ (2-BrC ₆ H ₄)	22.1	387.1	379.4
PhSCH ₂ (4-CF ₃ C ₆ H ₄)	100.5	384.4	376.7
PhSCH ₂ (3-CF ₃ C ₆ H ₄)	58.2	386.3	378.6
PhSCH ₂ (2-CF ₃ C ₆ H ₄)	20.2	386.2	378.5
PhSCH ₂ (3-CNC ₆ H ₄)	143.3	383.4	375.7
PhSCH ₂ (2-CNC ₆ H ₄)	324.0	382.2	374.6
PhSCH ₂ (4-CH ₃ OC ₆ H ₄)	0.05	398.9	390.9
PhSCH ₂ (3-CH ₃ OC ₆ H ₄)	1.1	392.9	385.1
PhSCH ₂ (4-CH ₃ C ₆ H ₄)	0.3	393.8	385.9
PhSCH ₂ (4-BNC ₆ H ₄) ^a	0.5	394.7	386.8
PhSCH ₂ (3-BNC ₆ H ₄) ^a	0.1	397.8	389.8
PhSCH ₂ (2-BNC ₆ H ₄) ^a	≅ 0 ^b	401.0	392.4

^a BN=6-butyl-(*N*-B)-1,3,6,2-dioxazaborocane.

^b The low conversion of PhSCH₂(2-BNC₆H₄) resulted in a high uncertainty when measuring the concentration precisely.

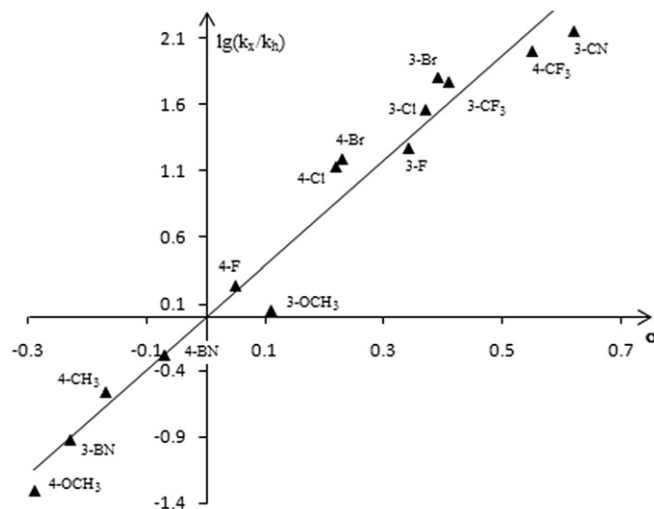


Fig. 1. The Hammett plot for benzylic deprotonation of a series of substituted benzyl-phenyl sulfides (XBPS).

electron withdrawing effect works, whereas the rate decrease for the *ortho* isomer is probably due to the steric hindrance, which is another important factor modulating deprotonations of $-\text{CF}_3$ substituted arenes. The highest rates of deprotonation were observed for the ABS containing a cyano group. This substituent exhibits a significant electron withdrawing property, however, the conjugation of the π orbital in this group with the π system of the benzene allows the extension of the negative charge toward nitrogen leading to additional stabilization. Recently we have reported the deactivating effect of the 6-butyl-(*N*-B)-1,3,6,2-dioxazaborocane substituent on benzylic lithiation.¹² The obtained values of the relative deprotonation rate constants revealed that this substituent can act as a σ donor, decreasing the rate of benzylic deprotonation in comparison to the reference compound, however, the steric hindrance seems to be the important factor modulating the reaction rate (Table 1).

3. Computational studies

Although the metalation reaction normally occurs ‘irreversibly’, the knowledge of the equilibrium acidity of selected hydrogen atoms can provide helpful information about substituent effects. However, the experimental techniques, which usually involve gas-phase methods, often suffer from inaccuracy and cannot be applied to non-volatile substances.¹³ On the other hand quantum-chemical computations give us tools for the comparison of the hydrogen acidity within the same group of compounds. As shown by Schlosser et al. acidity correlates with the calculated heterolytical proton dissociation energy (deprotonation energies).¹⁴ Such an approach has been recently successfully applied in the studies of the substituent direction effects in the lithiation of boronated thiophenes.¹⁵ It should be stressed that the values of deprotonation energies do not correspond to the real energies of lithiation processes and are only used for the comparison of acidities. The calculations have been performed on B3LYP¹⁶/aug-cc-pVDZ¹⁷ level of theory and all obtained values are deposited in Table 1. The correlation of the obtained values with the $\lg k_x/k_h$ (Fig. 2) reflects the general trend obtained using the Hammett equation: the increase in deprotonation rate corresponds with the increase in acidity of the benzylic hydrogen atoms (measured as deprotonation Gibbs energy). However, in the series of *meta* substituted ABS’s the deprotonation Gibbs energy value for a fluorine substituent deviates from the monotonic decrease observed for the other substituents. We are far from attributing these deviations to any electronic effects because we realize that the extended calculations including the other methods or basis sets should be performed in order to justify the obtained deprotonation enthalpies.

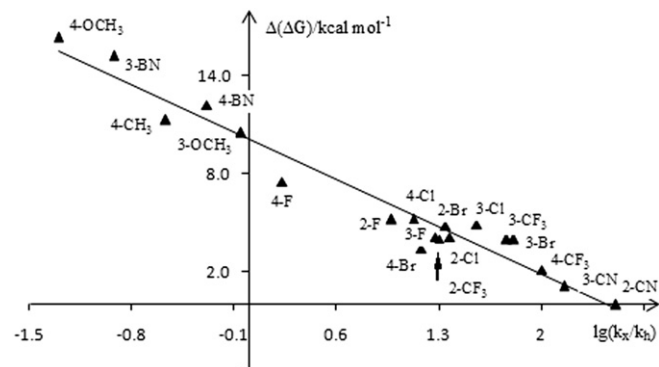
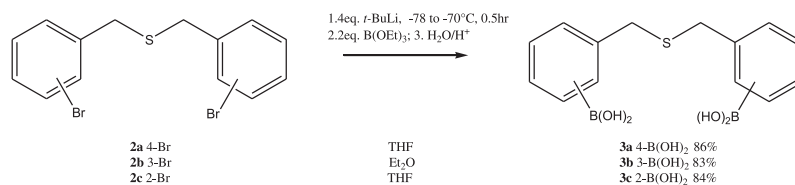


Fig. 2. A plot of the relative Gibbs energies for deprotonation of XPBS versus the relative rate constant of deprotonation.

4. Synthesis of diboronic acids

We next embarked on a study of di-lithiation via Br/Li exchange of a series of sulfides composed of two bromobenzene fragments linked via various carbon–sulfur chains: ($-\text{CH}_2-\text{S}-\text{CH}_2-$, $-\text{S}-\text{CH}_2-\text{S}-$, $-\text{S}-(\text{CH}_2)_3-\text{S}-$, $-\text{S}-(\text{CH}_2)_2-\text{S}-$, $-\text{S}-\text{CH}_2-$). Based on our previous results we expected that hydrogen atoms bonded to aliphatic carbon atoms in the studied compounds will be potentially reactive toward deprotonation. Thus, lithiation/boronation of **2a–c** was carried out in THF below -70°C using 4 equiv of *t*-BuLi. The usual workup afforded the respective diboronic acids **3a** and **3c** in high yields, whereas for **3b** the yield was decreased to 67% (Scheme 3). We attribute this result to competitive benzylic deprotonation. This is in agreement with the previous kinetic studies, which revealed that benzylic deprotonation is accelerated when the bromine atom is placed in the *meta* position. Although the benzylic positions in **2a–b** are also susceptible to

deprotonation, the Br/Li exchange occurs fast affording the respective aryllithium compounds. However, when the lithiation/borylation of **2b** was performed in diethyl ether, the yield of **3b** was similar as that for **3a** and **3c**.



Scheme 3. The synthesis of **3a–c**.

A similar protocol applied to **4a–c** resulted in formation of the respective diboronic acids **5a** and **5c** in high yields, whereas **5b** was obtained in only 58% yield. The explanation of the yield decrease relies on the competitive benzylic deprotonation as for the lithiation of **2b**. The replacement of THF with diethyl ether resulted in the quantitative formation of **5b** (Scheme 4). We turned next our attention to lithiation of **6a–c** (Scheme 5). As the methylene group adjacent to the two sulfur atoms in these compounds is highly susceptible to deprotonation, we decided to use diethyl ether in the synthesis of diboronic acids **7a–c**. Thus, the reaction of **6a** and **6b** with 4 equiv of *t*-BuLi, followed by treatment of the obtained organolithium derivatives with B(OEt)₃ afforded **7a–b** in moderate yields, which can be attributed to the competitive deprotonation of the –CH₂– group. However, the analogous reaction of **6c** afforded the respective boronic acid **7c** in only 26% yield. This product was contaminated with a significant amount of thiophenol (ca. 60%).

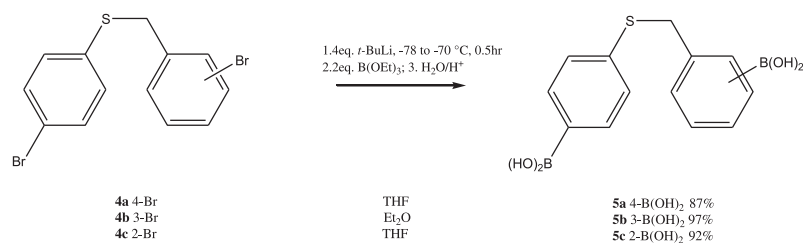
The formation of thiophenol can be reasonably explained by assuming that the transformation of **6c-Li₂** to **6c'-Li₂** proceeds via intramolecular –CH₂– deprotonation (Scheme 6). Quenching of **6c'-Li₂** with B(OEt)₃ afforded **7c-B₂**, which is unstable and undergoes the easy substitution at the α-carbon atom repelling the C₆H₅S[–] anion.¹⁸

This approach using *t*-BuLi/B(OEt)₃ in THF was thought to be effective in the preparation of diboronic acids **9** and **11a–c**. We expected that **8** and **10a–c** containing –CH₂CH₂– or –CH₂CH₂CH₂– linkers would give stable organo-dilithium intermediates. Thus,

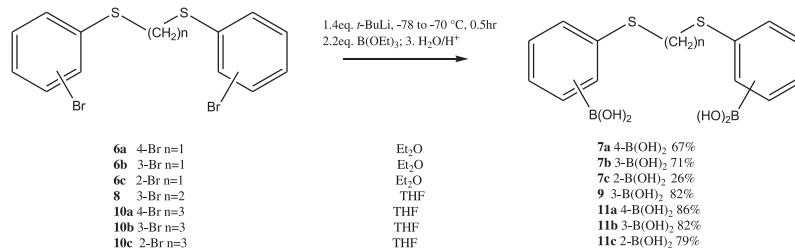
lithiation of these compounds using 4 equiv of *t*-BuLi and subsequent borylation with B(OEt)₃ afforded the respective diboronic acids **9** and **11a–c** in high yield.

5. X-ray studies

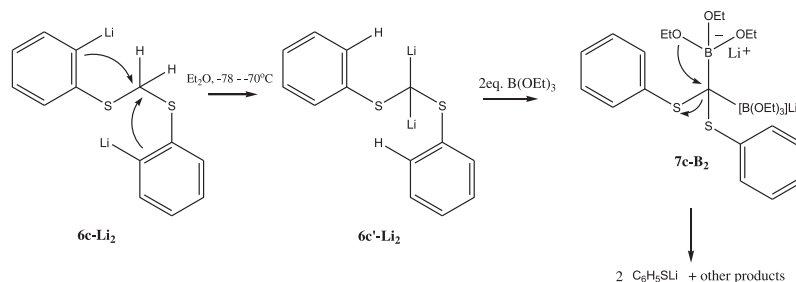
The formation of diboronic acid **7c** was confirmed by single crystal X-ray diffraction. To the best of our knowledge, this is the first crystal structure of a diboronic acid, where aromatic rings bearing –B(OH)₂ groups are connected via a linker with a sulfur atom. The obtained data revealed that **7c** belongs to the monoclinic *P*2₁/*c* space group. Views of the molecular structure together with the atom labeling scheme are depicted in Fig. 3. The asymmetric part of the unit cell contains two molecules of diboronic acid (**7c(I)** and **7c(II)**), which form a hydrogen-bonded R₂²(8) dimer (**7c(I)**–**7c(II)**), (O1–H27···O5 and O6–H32···O2 contacts). Additionally, the *anti*-conformed hydroxyl groups are arranged in intramolecular hydrogen interaction with sulfur atoms (O2–H28···S1 and O5–H31···S3). The geometrical parameters of the hydrogen bonds are given in the Supplementary data. In general, the molecular geometries of **7c(I)** and **7c(II)** are very similar. The aromatic ring planes within the same molecules are parallel to each other, and



Scheme 4. The synthesis of **5a–c**.



Scheme 5. The synthesis of **7a–c**, **9**, and **11a–c**.



Scheme 6. The proposed mechanism of thiophenol formation on lithiation of **6c**.

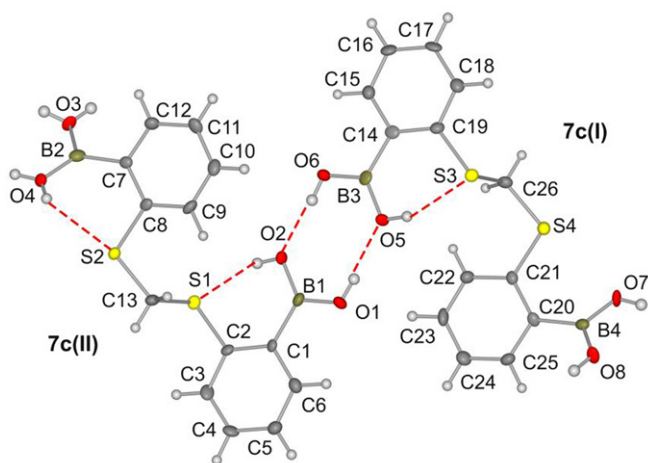


Fig. 3. Labeling of atoms and estimation of their atomic thermal motion as ADPs (50% probability level) for **7c**. Hydrogen interactions are shown as red dashed lines. Selected bond lengths (Å) and angles (°): B1–O1 1.366(1), B1–O2 1.363(1), B1–C1 1.559(1), O2–B1–O1 116.71(4), O2–B1–C1–C2 –42.96(11), B2–O4 1.382(1), B2–O3 1.353(1), B2–C7 1.580(1), O4–B2–O3 118.31(5), O4–B2–C7–C8 5.48(12). Crystallographic data for this structure has been deposited with the Cambridge Crystallographic Data Centre as supplementary publication number CCDC 893237.

conformation, in **7c(II)** molecule the *syn–anti* conformations is only observed for –B(OH)_2 group bonded to C1.

For the second –B(OH)_2 group (bonded to the C7 atom), the residual density map reveals that hydrogen atoms are in disorder. The molecules of **7c(I)** and **7c(II)** are also arranged in different structural motifs. Hydrogen-bonded $R_2^2(8)$ dimers are formed between molecules of **7c(I)** (O7–H33...O8). These **7c(I)–7c(I)** dimers are joined to chains by lateral hydrogen interactions (O8–H34...O7) within the $R_4^4(8)$ motifs (Fig. 4). Such hydrogen interaction is commonly observed for the structure of boronic and diboronic acids.¹⁹ In contrast, the molecules of **7c(II)** are mutually displaced—each molecule interacts with two neighbors via a single hydrogen interaction (O3–H29A...O4, O4–H30A...O4) forming chains with an alternating sequence of molecules (motif $R_3^3(8)$). Both types of chain are parallel to the [101] direction and together connect molecules of **7c(I)** and **7c(II)** into a 2-dimensional sheet (Fig. 4). We also found that –B(OH)_2 groups, which participate in the dimeric **7c(I)–7c(II)** interactions are almost coplanar with the aromatic ring planes, while two other –B(OH)_2 groups are significantly twisted along the B–C bond with a dihedral angle close to 40°. The interactions between sheets are dominated by the weak contacts, from which the C–H...S ($d_{C3...S4}=3.569(3)$, symmetry operation: $1-x, 1-y, -z$) and C–H... π ($d_{C11...C11}=3.56(2)$, symmetry operation: $1-x, 0.5-y, 0.5-z$) should be mentioned.

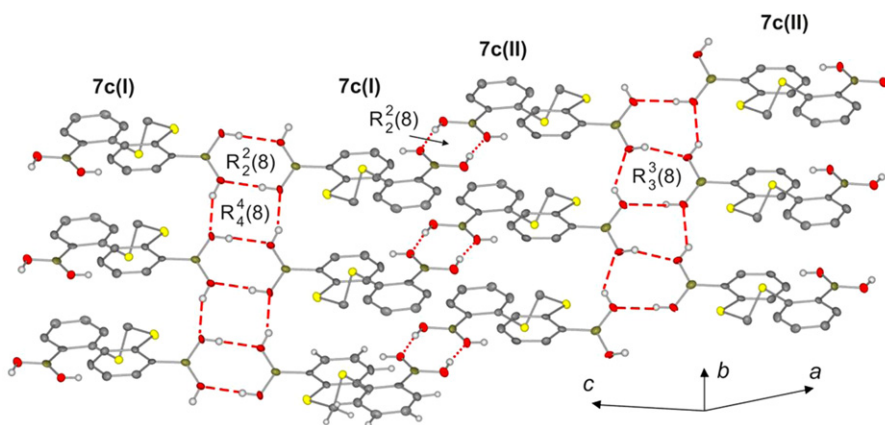


Fig. 4. 2D hydrogen-bonded layer with the illustration of selected crystal motifs. Hydrogen bonds are shown as red, dashed lines. Aromatic and methylene hydrogen atoms are omitted for clarity.

also remain parallel to the rings from the second independent molecule. The main difference between **7c(I)** and **7c(II)** occurs in the conformation of the –B(OH)_2 groups, regarding proton position within those groups. While, both –B(OH)_2 groups in **7c(I)** (bound to C14 and C20 carbon atoms) adopt a well-established *syn–anti*

6. Conclusions

We have developed an efficient method for the generation of useful di-lithiated aryl-alkyl sulfides, which were successfully employed in the synthesis of new diboronic acids. The selectivity of

the Br/Li exchange depends on the acidity of the hydrogen atoms in the aliphatic position. For the hydrogen atoms in the benzylic position the acidity is strongly influenced by the substituent in the benzene ring. The non-benzylic hydrogen atoms in the α position to sulfur are rather unreactive toward deprotonation with *t*-BuLi in THF at -78°C , unless they are flanked by two sulfur atoms. These studies were complemented by kinetic experiments, which compared the electronic and steric factors caused by substituents on the benzylic deprotonation rate. Theoretical calculations supported the observation that the benzylic deprotonation rate in the studied ABS is strongly dependent on the acidity of the benzylic hydrogen. The X-ray analysis of **7c** revealed the existence of three different structural motifs, which stabilize the structure by hydrogen bonding formation.

7. Experimental section

7.1. General

^1H and ^{13}C NMR spectra were recorded at room temperature on a Bruker 400 MHz spectrometer. Chemical shifts are given in parts per million relative to TMS in ^1H and ^{13}C NMR spectra. IR spectra were recorded on a Specord M80 spectrometer. Elemental analyzes were run with a VARIO ELIII apparatus. All analyzes were carried out at the Analytical Unit of the Chemistry Department, Warsaw University of Technology. All chemicals were received from Aldrich. THF and Et_2O were stored over sodium prior to use. All reactions were carried out under dry argon using standard Schlenk techniques. Melting points were determined in Pyrex capillary tubes with MeL-Temp apparatus.

Competition kinetics: (a) Pairs of substrates BPS and XBPS (5 mmol each) were dissolved in tetrahydrofuran (30 mL) and Me_3SiCl (20 mmol) was added to the obtained solution. The obtained mixture was cooled to -78°C (internal temperature, acetone-dry ice bath) maintaining the stirring. (b) Preparation of LDA solution: THF (30 mL) and diisopropylamine (5 mmol, 0.70 mL) were placed into the Schlenk flask and the obtained solution was cooled to -78°C (internal temperature). A commercial solution of *n*-BuLi (5 mmol, 0.5 mL) in hexanes was added to diisopropylamine solution and the reaction mixture was stirred for 0.5 h. The obtained LDA was transferred rapidly via cannula to the stirred solution of substrates. The reaction mixture has been stirred at -78°C for 2 h. The cooling bath was removed and the reaction mixture was heated to ambient temperature. 2-Bromobenzoyloxy-2,6-difluorobenzene (1.49 g, 5 mmol) as the internal reference was added to the reaction mixture maintaining the stirring. The obtained solution was poured onto HCl(aq) (20%, 60 mL) and stirred for 15 min. The organic phase was extracted with diethyl ether (3 \times 30 mL) and the combined ether phases were dried over anhydrous MgSO_4 . The solvent was evaporated using water bath (ca. 50°C) and rotary vacuum pump. The obtained oil was analyzed by ^1H NMR spectroscopy. The peak areas of substrates BPS (c_{h}) and XBPS (c_{x}) relative to those of the internal standard ($c_{\text{o}}^{\text{x}} = c_{\text{o}}^{\text{h}}$) were listed and were used to calculate the rate ratios $k_{\text{x}}/k_{\text{h}}$. In each case it was ascertain that the consumption of substrates BPS and XBPS was counterbalanced by the formation of silylated products in corresponding quantities.

Error estimation: on the basis of numerous repetitive experiments we assume the relative rates $k_{\text{x}}/k_{\text{h}}$ to be afflicted with an average error of less than 10% unless they are less than 1.0.

7.2. Lithiation procedures

7.2.1. Bis-(4-dihydroxyborylbenzyl)sulfide (3a). A solution of bis-(4-bromobenzyl)sulfide **2a** (3.7 g, 0.01 mol) in THF (20 mL) was added to a stirred solution of *t*-BuLi (1.7 M, 24 mL, 0.04 mol) in THF

(60 mL) at -70°C . The obtained yellow slurry was stirred for 0.5 h at -70°C followed by the dropwise addition of $\text{B}(\text{OEt})_3$ (2.92 g, 0.02 mol). The mixture was stirred for 1 h and then quenched with HCl(aq) (10%, 50 mL). The resultant solution was extracted twice with diethyl ether (2 \times 50 mL) and the obtained organic phase was dried over anhydrous MgSO_4 . The ethereal solution was filtered and the solvent was evaporated under reduced pressure. Water (100 mL) was added to the obtained precipitate. The crude product was separated by filtration, washed with hexane (50 mL) and dried to give **3a** as a colorless powder; yield 2.60 g (86%), $\text{mp} > 200^\circ\text{C}$; ν_{max} (KBr) 3360 (br), 1594, 1510, 1354, 1263, 1115, 1020, 1006, 850, 821, 774, 724, 644, 625, 510 cm^{-1} ; ^1H NMR (400 MHz, acetone- d_6 + D_2O): δ 7.78 (4H, d, $J=8.0$ Hz, Ar), 7.24 (4H, d, $J=8.0$ Hz, Ar), 3.61 (4H, s, $-\text{CH}_2-$); $^{13}\text{C}\{^1\text{H}\}$ NMR (100.6 MHz, acetone- d_6 + D_2O): 140.42, 134.21, 127.99, 35.2. Anal. Calcd for $\text{C}_{14}\text{H}_{16}\text{B}_2\text{O}_4\text{S}$: C, 55.69, H, 5.34. Found: C, 55.76, H, 5.43.

7.2.2. Bis-(3-dihydroxyborylbenzyl)sulfide (3b). The product was prepared as described for **3a** starting with **2b** (3.72 g, 0.01 mol) and using diethyl ether (150 mL) as the solvent; yield 2.50 g (83%), colorless powder, $\text{mp} > 190^\circ\text{C}$; ν_{max} (KBr) 3296 (br), 1600, 1484, 1420, 1349, 1280, 1236, 1208, 1176, 1160, 1100, 1076, 1028, 808, 708, 656, 564, 452 cm^{-1} ; ^1H NMR (400 MHz, acetone- d_6): δ 7.81 (2H, s, Ar), 7.75–7.72 (2H, m, Ar), 7.37–7.34 (2H, m, Ar), 7.28 (2H, t, $J=7.0$ Hz, Ar), 3.66 (4H, s); $^{13}\text{C}\{^1\text{H}\}$ NMR (100.6 MHz, acetone- d_6): 138.25, 135.60, 133.47, 131.66, 128.33, 36.53. Anal. Calcd for $\text{C}_{14}\text{H}_{16}\text{B}_2\text{O}_4\text{S}$: C, 55.69, H, 5.34. Found: C, 55.79, H, 5.16.

7.2.3. Bis-(2-dihydroxyborylbenzyl)sulfide (3c). The product was prepared as described for **3a** starting with **2c** (3.72 g, 0.01 mol); yield 2.54 g (84%), colorless powder, $\text{mp} > 138^\circ\text{C}$; ν_{max} (KBr) 3357 (br), 2954, 1587, 1564, 1464, 1423, 1341, 1253, 1145, 1060, 1014, 818, 761, 643, 589, 512, 494, 464, 417 cm^{-1} ; ^1H NMR (200 MHz, acetone- d_6): δ 7.58 (2H, d, $J=7.2$ Hz, Ar), 7.30–7.10 (6H, m, Ar), 3.90 (4H, s); $^{13}\text{C}\{^1\text{H}\}$ NMR (100.6 MHz, acetone- d_6): 143.81, 135.26, 130.24, 129.89, 126.75, 36.98. Anal. Calcd for $\text{C}_{14}\text{H}_{16}\text{B}_2\text{O}_4\text{S}$: C, 55.69, H, 5.34. Found: C, 55.70, H, 5.54.

7.2.4. (4-Dihydroxyborylphenyl)(4-dihydroxyborylbenzyl)sulfide (5a). The product was prepared as described for **3a** starting with **4a** (3.58 g, 0.01 mol); yield 2.51 g (87%), colorless powder, $\text{mp}=256^\circ\text{C}$; ν_{max} (KBr) 3363 (br), 1596, 1512, 1352, 1268, 1116, 1020, 1004, 848, 820, 772, 728, 648, 628, 512 cm^{-1} ; ^1H NMR (400 MHz, acetone- d_6 + D_2O): δ 7.78 (2H, d, $J=8.0$ Hz, Ar), 7.74 (2H, d, $J=8.4$ Hz, Ar), 7.35 (2H, d, $J=8.0$ Hz, Ar), 7.28 (2H, d, $J=8.4$ Hz, Ar), 4.24 (2H, s, $-\text{CH}_2-$); $^{13}\text{C}\{^1\text{H}\}$ NMR (100.6 MHz, acetone- d_6 + D_2O): 140.35, 140.19, 135.42, 135.08, 128.74, 127.67, 37.60. Anal. Calcd for $\text{C}_{13}\text{H}_{14}\text{B}_2\text{O}_4\text{S}$: C, 54.23, H, 4.90. Found: C, 54.12, H, 4.98.

7.2.5. (4-Dihydroxyborylphenyl)(3-dihydroxyborylbenzyl)sulfide (5b). The product was prepared as described for **3a** starting with **4b** (3.58 g, 0.01 mol) and using diethyl ether (120 mL) as the solvent; yield 2.79 g (97%), colorless powder, $\text{mp}=239^\circ\text{C}$; ν_{max} (KBr) 3299 (br), 1653, 1596, 1544, 1488, 1350, 1180, 1108, 1036, 1012, 984, 816, 728, 704, 648, 628, 504, 450, 428 cm^{-1} ; ^1H NMR (400 MHz, acetone- d_6 + D_2O): δ 7.89 (1H, s, Ar), 7.75–7.71 (3H, m, Ar), 7.44–7.42 (1H, m, Ar), 7.30–7.24 (3H, m, Ar), 4.23 (2H, s, $-\text{CH}_2-$); $^{13}\text{C}\{^1\text{H}\}$ NMR (100.6 MHz, acetone- d_6 + D_2O): 140.60, 137.21, 135.67, 135.52, 133.85, 131.58, 128.45, 127.57, 37.79. Anal. Calcd for $\text{C}_{13}\text{H}_{14}\text{B}_2\text{O}_4\text{S}$: C, 54.23, H, 4.90. Found: C, 53.90, H, 5.02.

7.2.6. (4-Dihydroxyborylphenyl)(2-dihydroxyborylbenzyl)sulfide (5c). The product was prepared as described for **3a** starting with **4c** (3.58 g, 0.01 mol); yield 2.65 g (92%), colorless powder, $\text{mp}=242^\circ\text{C}$; ν_{max} (KBr) 3393 (br), 3061, 1592, 1340, 1185, 1098, 736, 688 cm^{-1} ; ^1H

NMR (400 MHz, acetone- d_6): δ 7.74 (2H, d, $J=8.0$ Hz, Ar), 7.64 (1H, dd, $J=7.2, 1.6$ Hz, Ar), 7.32–7.27 (3H, m, Ar), 7.24 (1H, td, $J=7.2, 1.6$ Hz, Ar), 7.16 (1H, td, $J=7.2, 1.6$ Hz, Ar), 4.53 (2H, s, $-\text{CH}_2-$); ^{13}C { ^1H } NMR (100.6 MHz, acetone- d_6): 142.75, 140.87, 135.31, 130.07, 129.99, 127.59, 126.93, 37.63. Anal. Calcd for $\text{C}_{13}\text{H}_{14}\text{B}_2\text{O}_4\text{S}_2$: C, 54.23, H, 4.90. Found: C, 53.87, H, 5.02.

7.2.7. *Bis-(4-dihydroxyborylphenylthio)methane (7a)*. A solution of bis-(4-bromobenzylthio)methane **6a** (3.9 g, 0.01 mol) in Et_2O (60 mL) was added dropwise to a stirred solution of *t*-BuLi (1.7 M, 24 mL, 0.04 mol) in Et_2O (150 mL) at -70°C . The obtained yellowish precipitate was stirred for 0.5 h at -70°C followed by the dropwise addition of $\text{B}(\text{OEt})_3$ (2.92 g, 0.02 mol). The mixture was stirred for 1 h and then quenched with HCl aq (10%, 50 mL). The organic phase was separated and dried over anhydrous MgSO_4 . The ethereal solution was filtered and the solvent was evaporated under reduced pressure. Water (100 mL) was added to the obtained precipitate. The crude product was separated by filtration, washed with hexane (2 \times 50 mL) and dried to give **7a** as a colorless powder; yield 2.14 g (67%), mp $>260^\circ\text{C}$; ν_{max} (KBr) 3221 (br), 2516, 2262, 1596, 1472, 1393, 1197, 1116, 1020, 1004, 812, 725 cm^{-1} ; ^1H NMR (400 MHz, acetone- d_6): δ 7.81 (4H, d, $J=8.4$ Hz, Ar), 7.38 (4H, d, $J=8.4$ Hz, Ar), 4.61 (2H, s, $-\text{CH}_2-$); ^{13}C { ^1H } NMR (100.6 MHz, acetone- d_6): 138.70, 135.57, 128.59, 37.47. Anal. Calcd for $\text{C}_{13}\text{H}_{14}\text{B}_2\text{O}_4\text{S}_2$: C, 48.79, H, 4.41. Found: C, 48.76, H, 4.50.

7.2.8. *Bis-(3-dihydroxyborylphenylthio)methane (7b)*. The product was prepared as described for **7a** starting with **6b** (3.9 g, 0.01 mol); yield 2.26 g (71%), colorless powder, mp $>248^\circ\text{C}$; ν_{max} (KBr) 3358 (br), 1585, 1564, 1474, 1410, 1345, 1255, 1163, 1135, 1094, 1026, 882, 814, 794, 724, 702, 586, 514 cm^{-1} ; ^1H NMR (400 MHz, acetone- d_6 + D_2O): δ 7.92 (2H, s, Ar), 7.74–7.72 (2H, m, Ar), 7.50–7.47 (2H, m, Ar), 7.30 (2H, t, $J=7.6$ Hz, Ar), 4.53 (2H, s, $-\text{CH}_2-$); ^{13}C { ^1H } NMR (100.6 MHz, acetone- d_6 + D_2O): 140.44, 140.26, 135.42, 135.10, 128.78, 127.77, 37.68. Anal. Calcd for $\text{C}_{13}\text{H}_{14}\text{B}_2\text{O}_4\text{S}_2$: C, 48.79, H, 4.41. Found: C, 48.62, H, 4.50.

7.2.9. *Bis-(2-dihydroxyborylphenylthio)methane (7c)*. The product was prepared as described for **7a** starting with **6c** (3.9 g, 0.01 mol); yield 0.83 g (26%), colorless powder, mp = 114–115 $^\circ\text{C}$; ν_{max} (KBr) 3362 (br), 1584, 1560, 1464, 1428, 1340, 1252, 1141, 1056, 1012, 816, 760, 644, 588, 508, 492, 460, 416 cm^{-1} ; ^1H NMR (400 MHz, acetone- d_6 + D_2O): δ 7.66 (2H, dd, $J=7.2, 1.6$ Hz, Ar), 7.53 (2H, dd, $J=7.2, 0.8$ Hz, Ar), 7.35 (2H, td, $J=7.6, 1.6$ Hz, Ar), 7.26 (2H, td, $J=7.2, 0.8$ Hz, Ar), 4.46 (2H, s, $-\text{CH}_2-$); ^{13}C { ^1H } NMR (100.6 MHz, acetone- d_6 + D_2O): 139.12, 135.36, 132.74, 130.84, 127.64, 43.10. Anal. Calcd for $\text{C}_{13}\text{H}_{14}\text{B}_2\text{O}_4\text{S}_2$: C, 48.79, H, 4.41. Found: C, 48.71, H, 4.52.

7.2.10. *1,2-[Bis-(3-dihydroxyborylphenylthio)]ethane (9)*. The product was prepared as described for **3a** starting with **8** (4.04 g, 0.01 mol); yield 2.74 g (82%), colorless powder, mp $>200^\circ\text{C}$; ν_{max} (KBr) 3265 (br), 1592, 1560, 1480, 1432, 1400, 1341, 1192, 1120, 1035, 777, 704 cm^{-1} ; ^1H NMR (400 MHz, acetone- d_6): δ 7.86 (2H, d, $J=1.6$ Hz, Ar), 7.70 (2H, dt, $J=7.2, 1.6$ Hz, Ar), 7.36 (2H, dq, $J=7.2, 1.6, 1.2$ Hz, Ar), 7.28 (2H, t, $J=7.2$ Hz, Ar), 3.14 (4H, s, $-\text{CH}_2\text{CH}_2-$); ^{13}C { ^1H } NMR (100.6 MHz, acetone- d_6): 136.24, 135.28, 133.00, 132.12, 129.17, 33.77. Anal. Calcd for $\text{C}_{14}\text{H}_{16}\text{B}_2\text{O}_4\text{S}_2$: C, 50.34, H, 4.83. Found: C, 50.21, H, 4.91.

7.2.11. *1,3-[Bis-(4-dihydroxyborylphenylthio)]propane (11a)*. The product was prepared as described for **3a** starting with **10a** (4.18 g, 0.01 mol); yield 2.99 g (86%), colorless powder, mp $>156^\circ\text{C}$; ν_{max} (KBr) 3300 (br), 2912, 2414, 1592, 1544, 1496, 1352, 1184, 1102, 1028, 1008, 820, 732, 644, 628, 512, 496, 444 cm^{-1} ; ^1H NMR (400 MHz, acetone- d_6 + D_2O): δ 7.76 (4H, d, $J=8.4$ Hz, Ar), 7.28 (4H, d, $J=8.4$ Hz, Ar), 3.14 (4H, t, $J=7.2$ Hz, S- CH_2-), 1.93 (2H, q, $J=7.2$ Hz, C- CH_2-C);

^{13}C { ^1H } NMR (100.6 MHz, acetone- d_6 + D_2O): 139.81, 135.56, 127.61, 31.42. Anal. Calcd for $\text{C}_{15}\text{H}_{18}\text{B}_2\text{O}_4\text{S}_2$: C, 51.76, H, 5.21. Found: C, 51.86, H 5.31.

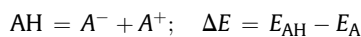
7.2.12. *1,3-[Bis-(3-dihydroxyborylphenylthio)]propane (11b)*. The product was prepared as described for **3a** starting with **10b** (4.18 g, 0.01 mol); yield 2.85 g (82%), colorless powder, mp $>87^\circ\text{C}$; ν_{max} (KBr) 3403 (br), 3304 (br), 2928, 1584, 1564, 1472, 1406, 1344, 1256, 1168, 1136, 1092, 1028, 880, 812, 792, 724, 700, 588, 518 cm^{-1} ; ^1H NMR (400 MHz, acetone- d_6): δ 7.84 (2H, s, Ar), 7.66 (2H, dt, $J=7.6, 1.0$ Hz, Ar), 7.38 (2H, dq, $J=7.6, 1.0, 0.6$ Hz, Ar), 7.26 (2H, t, $J=7.6$ Hz, Ar), 3.09 (4H, t, $J=7.2$ Hz, S- CH_2-), 1.89 (2H, q, $J=7.2$ Hz, C- CH_2-C); ^{13}C { ^1H } NMR (100.6 MHz, acetone- d_6): 136.03, 135.52, 132.52, 131.56, 128.99, 32.36. Anal. Calcd for $\text{C}_{15}\text{H}_{18}\text{B}_2\text{O}_4\text{S}_2$: C, 51.76, H, 5.21. Found: C, 51.78, H, 5.24.

7.2.13. *1,3-[Bis-(2-dihydroxyborylphenylthio)]propane (11c)*. The product was prepared as described for **3a** starting with **10c** (4.18 g, 0.01 mol); yield 2.75 g (79%), colorless powder, mp = 177–178 $^\circ\text{C}$; ν_{max} (KBr) 3362 (br), 2956, 2920, 1584, 1560, 1464, 1428, 1340, 1252, 1141, 1056, 1012, 816, 760, 644, 588, 508, 492, 460, 416 cm^{-1} ; ^1H NMR (400 MHz, acetone- d_6): δ 7.73 (2H, dd, $J=8.0, 1.6$ Hz, Ar), 7.42 (2H, dd, $J=8.0, 1.2$ Hz, Ar), 7.33 (2H, td, $J=8.0, 1.6$ Hz, Ar), 7.25 (2H, td, $J=8.0, 1.2$ Hz, Ar), 3.03 (4H, t, $J=7.2$ Hz, S- CH_2-), 1.83 (2H, q, $J=7.2$ Hz, C- CH_2-C); ^{13}C { ^1H } NMR (100.6 MHz, acetone- d_6): 139.88, 135.89, 133.11, 131.09, 127.45, 35.27. Anal. Calcd for $\text{C}_{15}\text{H}_{18}\text{B}_2\text{O}_4\text{S}_2$: C, 51.76, H, 5.21. Found: C, 51.58, H, 5.03.

X-ray data: The single crystal X-ray measurements were performed on a Kuma KM4CCD κ -axis diffractometer with graphite-monochromated MoK_α radiation ($\lambda=0.71073$ Å) and equipped with an Oxford Cryosystems nitrogen gas-flow apparatus. The crystal was positioned at 50 mm from the KM4CCD camera. The data were corrected for Lorentz and polarization effects. Data reduction and analysis were carried out with the Oxford Diffraction Ltd. suite of programs.²⁰ All structures were solved by direct methods using SHELXS-97 and refined using SHELXL-97.²¹ All non-hydrogen atoms were refined anisotropically. All hydrogen atoms were placed in calculated positions with C–H distance of 0.95 Å (phenyl), 0.99 Å (methylene) and O–H distance of 0.84 Å. They were visible in difference maps and they were included in the refinement in riding-motion approximation with U_{iso} (phenyl H) = 1.2 U_{eq} (C), U_{iso} (methylene H) = 1.5 U_{eq} (C) and U_{iso} (hydroxyl H) = 1.5 U_{eq} (O). $\text{C}_{26}\text{H}_{19}\text{B}_4\text{O}_8\text{S}_4$; molecular weight, 320.00 a.u.; $T=100(2)$ K; monoclinic space group, $P2_1/c$; unit cell dimensions, $a=24.446(2)$ Å, $b=5.073(1)$ Å, $c=24.734(2)$ Å, $\beta=106.84(1)^\circ$, $V=2935.9(3)$ Å³; $Z=8$; $d_{\text{calcd}}=1.448$ g cm^{-3} ; absorption coefficient, $\mu=0.372$ mm⁻¹; $F(000)=1328$; crystal size, 0.10 mm \times 0.10 mm \times 0.07 mm; θ range for data collection: 2.05°–28.65°; index ranges: $-31 < h < 32$, $-6 < k < 6$, $-33 < l < 32$; reflections collected: 23,191/unique: 3611 ($R_{\text{int}}=0.0324$); absorption correction—multi-scan; refinement method—full-matrix least-squares on F^2 ; goodness-of-fit on F^2 , $\text{GoF}=1.010$; data/restraints/parameters 3611/5/392; final R indices ($I > 2\sigma(I)$): $R1=0.0571$, $wR2=0.1116$; R indices (all data): $R1=0.1393$, $wR2=0.1642$; largest diffraction peak and hole: 0.52 and -0.50 e Å⁻³.

Computational details: All geometry optimizations and frequency calculations were carried out with GAUSSIAN09²² suite of programs and Becke-style three parameter density functional method using the Lee–Yang–Parr correlation functional (B3LYP).¹⁴ The aug-cc-pVDZ¹⁵ basis sets were used to calculate the optimal geometries. The minima were confirmed by vibrational frequency calculations within harmonic approximation (no imaginary frequencies). In optimization processes no symmetry constraints were applied.

Deprotonation energies were calculated according to the scheme:



where, ΔE is deprotonation energy, E_{AH} is the energy of the ABS molecule and E_A corresponds to the energy of a carbanion.

To establish the outcome of the quantum-chemical method we have performed additional calculation for PhSCH₂(2-FC₆H₄), PhSCH₂(3-FC₆H₄), and PhSCH₂(4-FC₆H₄) at the MP2²³/6-31+G(d)²⁴ and MP2/cc-pVTZ levels of theory, obtaining similar values of the deprotonation enthalpies [382.7 kJ mol⁻¹ and 379.45 kJ mol⁻¹, 380.2 kJ mol⁻¹ for MP2/6-31+G(d) method and 381.1 kJ mol⁻¹, 377.4 kJ mol⁻¹, and 378.9 kJ mol⁻¹ for MP2/cc-pVTZ].

Acknowledgements

This work was supported by the 'Iuventus Plus' program of the Polish Ministry of Science and Higher Education in the framework of project 0111/IP3/2011/71. The X-ray measurements of compound **7c** were undertaken at the Crystallographic Unit of the Physical Chemistry Laboratory, Chemistry Department, University of Warsaw. The authors thank the Interdisciplinary Centre for Mathematical and Computational Modeling in Warsaw for providing computational facilities (G33-14). Support from Aldrich Chemical Company, Milwaukee, WI, USA, through the donation of chemicals and equipment is gratefully acknowledged.

Supplementary data

Copies of ¹H and ¹³C NMR spectra of new compounds and hydrogen bond geometry of **7c**. Supplementary data related to this article can be found at <http://dx.doi.org/10.1016/j.tet.2013.02.075>.

References and notes

- Hall, D. G.; Ishiyara, T.; Miyaura, N.; Suzuki, A.; Yoshida, K.; Hayashi, T.; Cham, D. M. T.; Lam, P. Y. S.; Kennedy, J. W. J.; Batey, R. A.; Matteson, D. S.; Carboni, B.; Carreaux, F.; Ishihara, K.; Cho, B. T.; James, T. D.; Yang, W.; Gao, X.; Wang, B. In *Boronic Acids*; Hall, D. G., Ed.; Wiley: VCH: Weinheim, Germany, 2005.
- (a) Zhang, L.; Lin, T.; Pau, X.; Wang, W.; Liu, T. X. *J. Mater. Chem.* **2012**, *22*, 9861; (b) Yu, J. T.; Chen, Z.; Sun, J.; Huang, Z.-T.; Zheng, Q.-Y. *J. Mater. Chem.* **2012**, *22*, 5369; (c) Nokabayashi, K.; Oya, H.; Mori, H. *Macromolecules* **2012**, *45*, 3197; (d) Dogru, M.; Sonnauer, A.; Gavryushin, A.; Knochel, P.; Bein, T. *Chem. Commun.* **2011**, 1707; (e) Spittler, E. L.; Koo, B. T.; Novotney, J. L.; Colson, J. W.; Uribe-Romo, F. J.; Gutierrez, G. D.; Claney, P.; Dichtel, W. R. *J. Am. Chem. Soc.* **2011**, *133*, 19416; (f) Nishiyabu, R.; Kubo, Y.; James, T. D.; Fossey, J. S. *Chem. Commun.* **2011**, 1124; (g) Dienstmaier, J. F.; Gigler, A. M.; Goetz, A. J.; Knochel, P.; Bein, T.; Lyapin, A.; Reichlmaier, S.; Heckl, W. M.; Lackinger, M. *ACS Nano* **2011**, *5*, 9737; (h) Feng, X.; Chen, L.; Dong, Y.; Jiang, D. *Chem. Commun.* **2011**, 1979; (i) Kitabayashi, T.; Shiokawa, K.; Moriuchi, T. K. *Chem. Eng. J.* **2009**, *146*, 520; (j) Furukawa, H.; Yaghi, O. M. *J. Am. Chem. Soc.* **2009**, *131*, 8875.
- Cabiddu, S.; Melis, S.; Piras, P. P.; Sotgiu, F. *J. Organomet. Chem.* **1979**, *178*, 291.
- Klis, T.; Wesela-Bauman, W.; Serwatowski, J.; Zadrozna, M. *Tetrahedron Lett.* **2010**, *51*, 1685.
- Durka, K.; Gontarczyk, K.; Klis, T.; Serwatowski, J.; Wozniak, K. *Appl. Organomet. Chem.* **2012**, *26*, 287.
- Anderson, D. R.; Faibish, N. C.; Beak, P. J. *J. Am. Chem. Soc.* **1999**, *121*, 7553.
- Collum, D. B.; McNeil, A. J.; Ramirez, A. *Angew. Chem., Int. Ed.* **2007**, *46*, 3002.
- Jaffe, H. H. *Chem. Rev.* **1953**, *53*, 191.
- The approximation of the kinetic data with first, third and fractional (1.5) order equations did not show the linear fit to $\lg(k_x/k_h)=\rho\sigma$.
- Faigl, F.; Marzi, E.; Schlosser, M. *Chem.—Eur. J.* **2000**, *6*, 771.
- Castagnetti, E.; Schlosser, M. *Chem.—Eur. J.* **2002**, *8*, 799.
- Durka, K.; Klis, T.; Serwatowski, J.; Wozniak, K. *Appl. Organomet. Chem.* **2011**, *25*, 669.
- Büker, H. H.; Nibbering, N. M. M.; Espinoza, D.; Mongin, F.; Schlosser, M. *Tetrahedron Lett.* **1997**, *38*, 8519.
- Hyla-Kryspin, I.; Grimme, S.; Büker, H. H.; Nibbering, N. M. M.; Cottet, F.; Schlosser, M. *Chem.—Eur. J.* **2005**, *11*, 1251.
- Borowska, E.; Durka, K.; Luliński, S.; Serwatowski, J.; Wozniak, K. *Eur. J. Org. Chem.* **2012**, 2208.
- (a) Becke, D. *Phys. Rev. A* **1988**, *38*, 3098; (b) Lee, C.; Yang, W.; Parr, R. G. *Phys. Rev. B* **1988**, *37*, 785.
- Dunning, T. H. *J. Chem. Phys.* **1989**, *90*, 1007.
- Matesson, D. S. *Tetrahedron* **1998**, *54*, 10555.
- (a) Aakeröy, C. B.; Desper, J.; Levin, B. *CrystEngComm* **2005**, *7*, 102; (b) Cyrański, M. K.; Jezierska, A.; Klimentowska, P.; Panek, J. J.; Sporzyński, A. *J. Phys. Org. Chem.* **2008**, *21*, 472; (c) Maly, K. E.; Maris, T.; Wuest, J. D. *CrystEngComm* **2006**, *8*, 33; (d) Rodríguez-Cuamatzi, P.; Arillo-Flores, O. I.; Bernal-Uruchurtu, M. I.; Höpfl, H. *Cryst. Growth Des.* **2005**, *5*, 167; (e) Durka, K.; Jarzemska, K. N.; Kaminski, R.; Lulinski, S.; Serwatowski, J.; Wozniak, K. *Cryst. Growth Des.* DOI: 10.1021/cg3005272.
- CrysAlis CCD/CrysAlis RED, 171.33.66; Oxford Diffraction Ltd.: 2007.
- Sheldrick, G. M. *Acta Crystallogr.* **2008**, *A64*, 112.
- Frisch, M. J.; Trucks, G. W.; Schlegel, H. B.; Scuseria, G. E.; Robb, M. A.; Cheeseman, J. R.; Montgomery, J. A.; Vreven, T.; Kudin, K. N.; Burant, J. C.; Millam, J. M.; Iyengar, S. S.; Tomasi, J.; Barone, V.; Mennucci, B.; Cossi, M.; Scalmani, G.; Rega, N.; Petersson, G. A.; Nakatsuji, H.; Hada, M.; Ehara, M.; Toyota, K.; Fukuda, R.; Hasegawa, J.; Ishida, M.; Nakajima, T.; Honda, Y.; Kitao, O.; Nakai, H.; Klene, M.; Li, X.; Knox, J. E.; Hratchian, H. P.; Cross, J. B.; Bakken, V.; Adamo, C.; Jaramillo, J.; Gomperts, R.; Stratmann, R. E.; Yazyev, O.; Austin, A. J.; Cammi, R.; Pomelli, C.; Ochterski, J. W.; Ayala, P. Y.; Morokuma, K.; Voth, G. A.; Salvador, P.; Dannenberg, J. J.; Zakrzewski, V. G.; Dapprich, S.; Daniels, A. D.; Strain, M. C.; Farkas, O.; Malick, D. K.; Rabuck, A. D.; Raghavachari, K.; Foresman, J. B.; Ortiz, J. V.; Cui, Q.; Baboul, A. G.; Clifford, S.; Cioslowski, J.; Stefanov, B. B.; Liu, G.; Liashenko, A.; Piskorz, P.; Komaromi, I.; Martin, R. L.; Fox, D. J.; Keith, T.; Al-Laham, M. A.; Peng, C. Y.; Nanayakkara, A.; Challacombe, M.; Gill, P. M. W.; Johnson, B.; Chen, W.; Wong, M. W.; Gonzalez, C.; Pople, J. A. *Gaussian 03, Revision C.02*; Gaussian: Wallingford, CT, 2004.
- Møller, C.; Plesset, M. S. *Pure Appl. Chem.* **1934**, 618.
- Krishnan, R.; Binkley, J. S.; Seeger, R.; Pople, J. A. *J. Chem. Phys.* **1980**, *72*, 650.